TEST Engineering & Management

September/October 2020
ISSN: 0193-4120 Page No. 337-357

Experimental Spectra and Theoretical Investigations of 5-Chloro-2-Pyridinol

V.Tamilselvi[a] M. Arivazhagan[a*]
[a]Department of Physics, pioneer kumaraswamy college ,
Nagercoil 629003 , kanyakumari (Dt)Tamil nadu, India
[a*] PG and Research Department of Physics,. Govt. Arts College,Trichy-022.
(Affiliated to Bharathidasan University,Tiruchirappalli 620 024), ,Tamil nadu, India
[a*]Corresponding author. Tel.:+91 94431 89328.
*E-mail address:arivu.m3008@*gmail.com (M. Arivazhagan).

Article Info
Volume 83
Page Number: 198-218
Publication Issue:
September/October 2020

Article History
Article Received: *04 June 2020*
Revised: *18 July 2020*
Accepted: *20 August 2020*
Publication: *15 September 2020*

Abstract

FT-IR and FT- Raman spectra of 5-chloro-2-pyridinol (CP) are recorded in the region 4000–400 cm^{-1} and 3500–50 cm^{-1}, respectively. Molecular structure and vibrational frequencies of CP have been investigated by density functional theory (DFT) calculations using Becke's three parameter exchange functional combined with Lee–Yang–Parr correlation (B3LYP) and Hartree fock (HF) method employing 6-311++G(d,p) basis set. Calculations have been performed giving energies, optimized structure, harmonic vibrational frequencies, IR intensities and Raman activities. Raman and IR spectra of CP were recorded and complete assignment of the observed vibrational bands of CP have been proposed. The predicted first hyperpolarizability suggests that the title compound is an attractive object of non-linear optical properties. The calculated HOMO–LUMO energies shows that charge transfer occur within the molecule and their related molecular properties were also discussed. The theoretical FT-IR and FT-Raman spectra for the title compound have also been constructed.

Keywords*:* 5-chloro-2-pyridinol; HOMO-LUMO; NBO .

1. INTRODUCTION

The study of the vibrational spectra of substituted pyridine entices the attention of many spectroscopists due to their wide application in pharmacology and agro-chemistry. Pyridine heterocycles are a repeated moiety in many large molecules with interesting photo physical, electrochemical and catalytic applications [1-9]. They serve as a good anaesthetic agents and used in the preparation of drugs for certain brain diseases. These pharmaceutically

acceptable salts and the pre-drugs are used for the treatment (or) prevention of diabetic neuropathy [10-11]. The pharmaceutical development of nitro pyridine derivatives has received considerable attention, since they are fully employed as chiral nucleophilic catalysts in a wide range of asymmetric synthetic process [12]. The vibrational spectra of substituted pyridine claims to be for the subject several investigations [13-15]. More recently [16], FT-IR and FT-Raman spectra of nitro pyridine are reported together with the vibrational assignments of the normal modes. However, the detailed HF/B3LYP at 6-311++G(d,p) comparative studies on the complete FT-IR and FT-Raman spectra of 5-chloro-2-pyridinol (CP) are not been reported so far. In this study, molecular geometry, optimized parameters and vibrational frequencies are computed and the performance of the computational methods for *ab initio* (HF), and B3LYP at 6-311++G(d,p) basis sets are compared. These methods predict relatively, accurate molecular structure and vibrational spectra with moderate computational effort. In particular, for polyatomic molecules, the DFT methods lead to the prediction of more accurate molecular structure and vibrational frequencies than the conventional *ab initio* Hartree–Fock calculations. In DFT methods, Becke's three parameter exact exchange-functional (B3) [17] combined with gradient-corrected correlational functional of Lee, Yang and Parr (LYP) [18-19] are the best in predicting the results for molecular geometry and vibrational wavenumbers for moderately larger molecule. The optimized geometrical parameters, fundamental vibrational frequencies, IR intensity, Raman activity, atomic charges, dipole moment, force constants, depolarization ratio and other thermodynamic parameters and energy gap through HOMO and LUMO energy were calculated using the Gaussian 09W packages.

2. EXPERIMENTAL DETAILS

A compound under investigation namely 5-chloro-2-pyridinol (CP) was purchased from Lancaster Chemical Company (U.K.) which was used record the spectra without any further purification. The FT-IR spectrum of CP was measured in the region 4000-400 cm^{-1} was recorded with a BRUKER IFS 66V spectrophotometer using KBr pellet. The FT-Raman spectrum of the title compound was recorded in the region 3500-50 cm^{-1} with a BRUKER RFS 100/s 66 V spectrophotometer using KBr pellet technique. Raman module was equipped with Nd:YAG laser source operating at 1064 nm line width 150 mw power. The spectra was recorded with a scanning speed of 50 cm^{-1} min^{-1} of spectral width 4 cm^{-1}. The reported wave numbers are believed to be accurate within ± 1cm^{-1}.

3. COMPUTATIONAL DETAILS

Quantum chemical density functional theory calculations were carried out using the Gaussian09W program package [20] with HF and B3LYP functions combined with the standard 6-311++G(d,p) basis sets. The Cartesian representation of the theoretical force constants are computed at the optimized geometry by assuming C_1 point group symmetry.

Scaling of the force field was performed according to the SQM procedure using selective scaling in the natural internal coordinate representation. Transformation of the force field and the subsequent normal coordinate analysis (NCA) including the least squares

September/October 2020
ISSN: 0193-4120 Page No. 337-357

refinement of the scaling factors, and calculation of total energy distribution (TED) were done on a PC with the MOLVIB program (version 7.0-G77) written by Sundies [21-23].

From the intensity theory of Raman scattering [24-26], the relative Raman intensities (I_i) and Raman activities (Si) were calculated using the Gaussian 09W Program.

$$I_i = \frac{f(\nu_0-\nu_i)^4 Si}{\nu_i\left(1-\exp\left(-\frac{hc\nu_i}{kT}\right)\right)} \quad \ldots (1)$$

where ν_0 is the exciting frequency (in cm^{-1}), ν_i is the vibrational wave number of the i^{th} normal mode, h, c and k are fundamental constants, and f is the normalization factor for all peak intensities.

4. RESULTS AND DISCUSSION

4.1. Geometry Optimization

The molecular structure with the numbering scheme is shown in Fig. 1. Geometry optimization was performed on the compound yielding the C_1 symmetry.

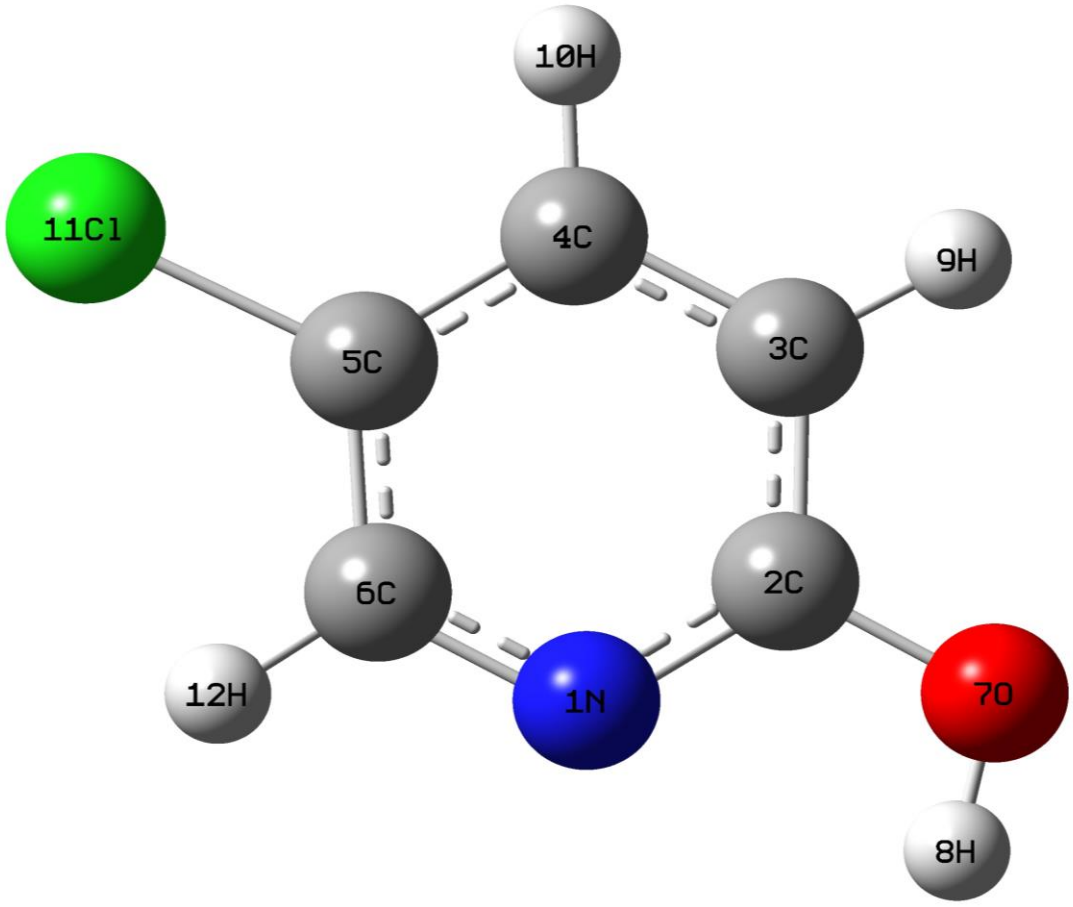

Fig. 1: Molecular structure of 5-chloro-2-pyridinol

Table 1 presents the optimized parameters, calculated at the selected two levels of theory namely HF/6-311++G (d,p) and B3LYP/6-311++G(d,p). Structural data provided in Table 1 indicates that various bond lengths are found to be almost the same at B3LYP/ 6-311++G (d,p) and HF/6-311++G (d,p) levels. A detailed description of vibrational modes can be given by means of normal coordinate analysis.

4.2. Vibrational Spectra

The title compound consists of 12 atoms and 30 normal modes of vibrations. All the vibrations are active both in the Raman scattering and infrared absorption. The vibrational frequencies are calculated for CP at *ab initio* and DFT (B3LYP) level using 6-311++G(d,p) basis set is collected in Table 2 along with the observed FT-IR and FT-Raman Spectral data. For visual comparison, the observed and calculated FT-IR and FT Raman spectra of CP at HF and DFT-B3LYP level using 6-311++G(d,p) basis set are shown in Figs. 2 and 3, respectively.

C-C vibrations

Benzene possesses six stretching vibrations of which the four with highest wave numbers occurring near 1650-1400 $cm^{-1}$are good group vibrations [27]. With heavy substituent's, the bonds tend to shift to slightly lower wave numbers and greater

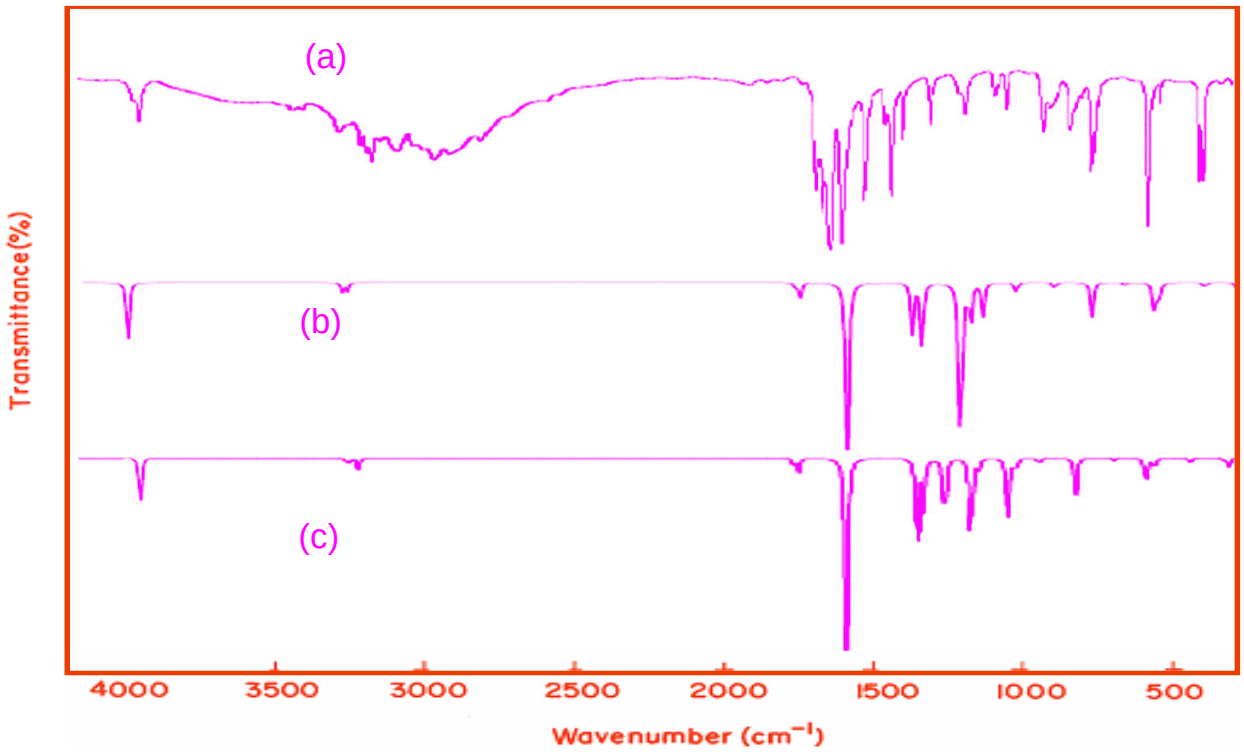

Fig. 2: Comparison of observed and calculated FTIR Spectra of 5-chloro-2-pyridinol (a) Observed (b) calculated with B3LYP/6-311++G(d,p) and (c) calculated with HF/6-311++G(d,p)

September/October 2020
ISSN: 0193-4120 Page No. 337-357

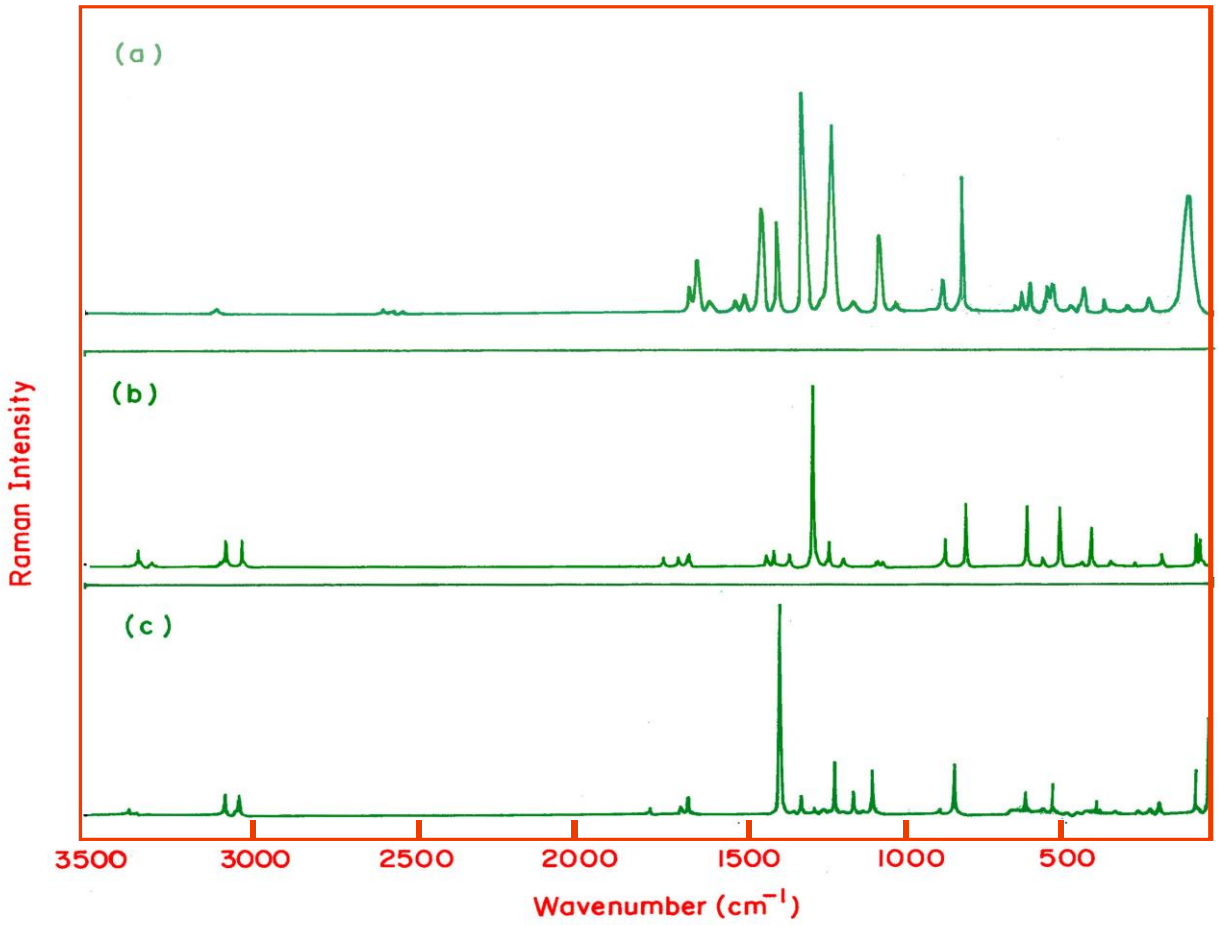

Fig. 3: Comparison of observed and calculated FT-Raman Spectra of 5-chloro-2-pyridinol (a) Observed (b) calculated with B3LYP/6-311++G(d,p) and (c) calculated with HF/6-311++G(d,p)

the number of substituents on the ring, broader are the absorption regions. In the title molecule, the FT-IR bands are observed at 1614, 1554, 992 cm^{-1} and 1621, 1548, 1040 and 826 cm^{-1} in FT-Raman are assigned to C-C stretching vibrations due to the substituents in benzene ring. The higher percentage of total energy distribution (TED) obtained for this group is encouraging and confirms the assignments proposed in this study for C-C stretching vibrations. The in-plane and out-of-plane bending vibrations of C-C group are also listed in Table 2.

C-H vibrations

The heteroaromatic structure shows the presence of C-H stretching vibrations in the region 3100-3000 cm^{-1} [28-30]. This is the characteristic region for the ready identification of C-H stretching vibrations. In this region, the bands are not affected appreciably by the nature of the substitutions. In the present investigation, the C-H stretching vibrations are observed at 3133, 3084 and 3057 cm^{-1} in the FT-IR spectrum and at 3130, 3084 and 3035 cm^{-1} in the

September/October 2020
ISSN: 0193-4120 Page No. 337-357

Raman for CP. The C-H in-plane and out-of-plane bending vibrations of the title compound are also identified and listed in Table 2.

O–H Vibrations

The precise positions of O-H band are dependent on the strength of hydrogen bond. The O-H stretching vibration is normally observed at about 3300 cm^{-1}. The O-H in-plane bending vibration is observed in the region 1440-1260 cm^{-1} [31-32]. In CP, the band appeared at 3700 cm^{-1} in FT-IR spectrum were assigned to O-H stretching modes of vibrations. The in-plane bending vibrations of hydroxy groups were identified at 1153, 1158 cm^{-1} in FT-IR and FT Raman respectively. O-H out-of-plane vibration of the title compound were identified and listed in Table 2.

C-Cl vibrations

The C–Cl stretching vibrations generally give strong bands in the region 760-505 cm^{-1} [32]. The FT-IR and FT-Raman bands observed at 638 cm^{-1} and 643 cm^{-1} are assigned to C-Cl stretching vibrations respectively. Most of the aromatic chloro compounds have a band of strong-to-medium intensity in the region 385-265 cm^{-1} due to C–Cl in-plane bending vibrations. Accordingly, the FT-Raman band identified at 244 cm^{-1} is assigned to the C–Cl in-plane bending mode. The C–Cl out of plane deformation vibration is established at 281 cm^{-1} in FT-Raman spectrum.

C-O vibrations

If a compound contains a carbonyl group, the absorption caused by C-O stretching is generally among the strongest present, occur in the region of 1260-1000 cm^{-1}. Hence, in the present investigation, the FT-Raman band at 1267 cm^{-1} is assigned to C–O stretching vibration of CP. The in-plane and out-of-plane vibrations of C–O group are presented in Table 2.

C–N vibrations

In aromatic compounds, the C–N stretching vibrations usually lie in the region 1400-1200 cm^{-1} [33]. In the present investigation, the FT-IR band appeared at 1426 and 1235 cm^{-1} and FT-Raman band appeared at 1426 cm^{-1} in CP are designated to C–N stretching vibrations. The in-plane and out-of-plane bending vibrations assigned in this study are also supported by the literature [34]. The identification of C–N vibration is a difficult task, since it falls in a complicated region of the vibrational spectrum. However, with the help of force field calculations, the C–N vibrations are identified and assigned in this task.

5. HOMO – LUMO BAND GAP

This electronic absorption corresponds to the transition from the ground to the first excited state, and is mainly described by one electron excitation from the highest occupied

molecular orbital (HOMO) to the lowest unoccupied molecular orbital (LUMO) [35]. Many organic molecules, containing conjugated π electrons, are characterized by large values of molecular first hyper polarizabilities, analyzed by means of vibrational spectroscopy. In most of the cases, even in the absence of inversion symmetry, the strongest band in the Raman spectrum is weak in the IR spectrum and vice-versa. But the intramolecular charge from the donor to acceptor group through a single-double bond conjugated, path can induce large variations of both the molecular dipole moment and the molecular polarizability, making IR and Raman activity strong at the same time. The experimental spectroscopic behavior described above is well accounted for DFT calculations in π conjugated system that predict exceptionally infrared intensities for the same normal modes. The analysis of the wave function indicates that the electron absorption corresponds to the transition from the ground to the first excited state and is mainly described by one-electron excitation from the highest occupied molecular orbital (HOMO) to the lowest unoccupied orbital (LUMO). The LUMO of π nature, (i.e. benzene ring) is delocalized over the whole C-C bond. The HOMO is located over benzene ring, iodine and the HOMO–LUMO transition implies an electron density transfer to the pyridine ring from hydroxyl group and chlorine atom. Moreover, the compositions of the frontier molecular orbital for CP are shown in Fig. 4.

September/October 2020
ISSN: 0193-4120 Page No. 337-357

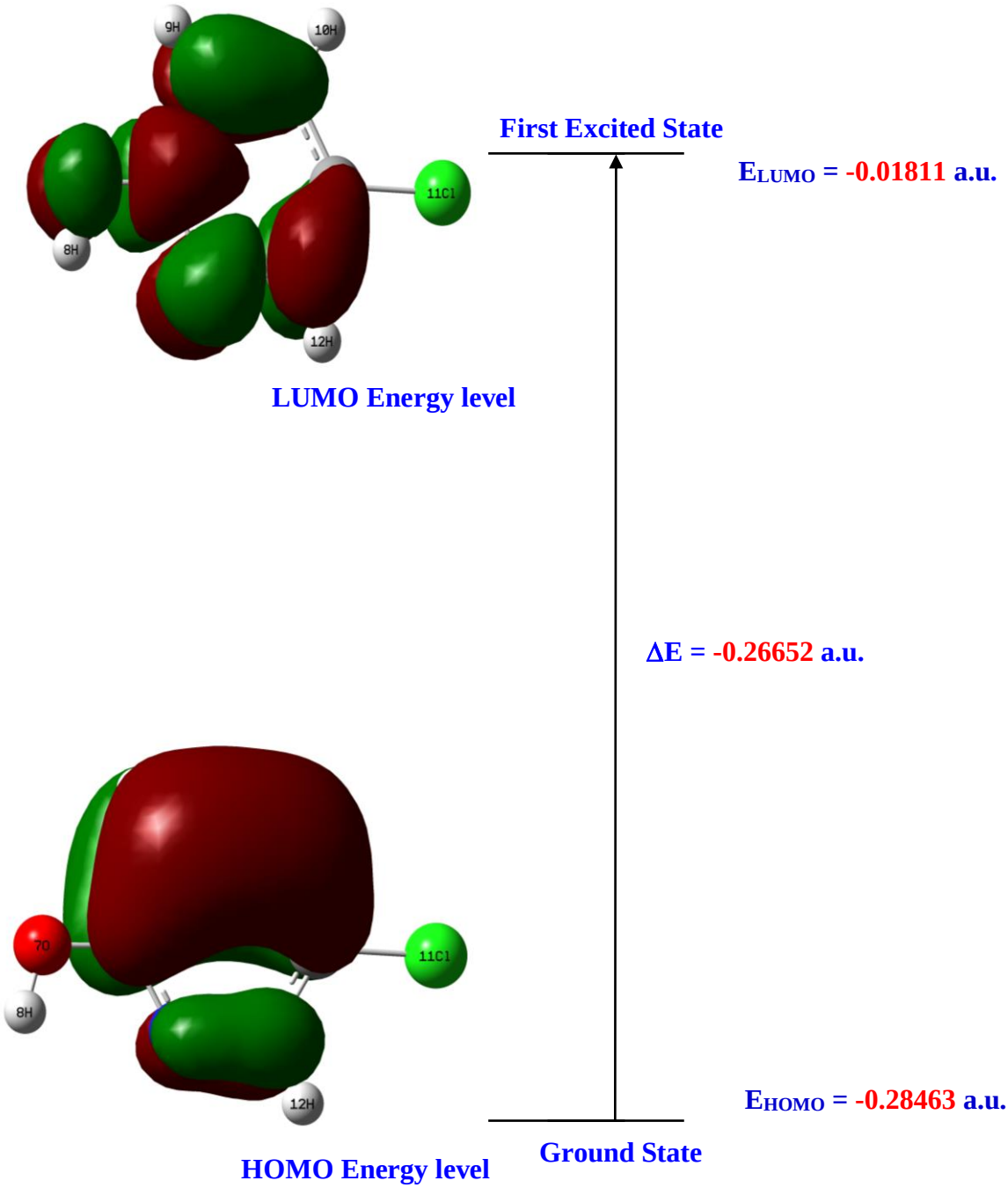

Fig. 4: HOMO-LUMO energy gap of 5-chloro-2-pyridinol by B3LYP/ 6-311++G(d,p)

September/October 2020
ISSN: 0193-4120 Page No. 337-357

The HOMO-LUMO energy gap of CP is calculated at B3LYP/6-311++G(d,p) level, which reveals that the energy gap reflects the chemical activity of the molecule. The LUMO as an electron acceptor (EA), represents the ability to obtain an electron and HOMO represents ability to donate an electron (ED). The ED groups to the efficient EA groups are linked through π-conjugated path.

The strong charge transfer interaction through π-conjugated bridge results in substantial ground state Donor-Acceptor (DA) mixing and the appearance of a charge transfer band in the electron absorption spectrum.

HOMO energy = -0.28463 a.u
LUMO energy = -0.01811a.u.
HOMO-LUMO energy gap = -0.26652 a.u.

The calculated self-consistent field (SCF) energy or optimized global minimum energy of CP is -783.233 Hartrees at B3LYP/6-311++G(d,p) and -780.573 Hartrees at HF/6-311++G(d,p) methods. The calculated HOMO, LUMO and other related properties at B3LYP/6-311++G(d,p) and HF/6-311++G(d,p) levels are listed in Table.3. The HOMO and LUMO energy gap explains the fact that eventual charge transfer interaction is takes place within the molecule. Gauss-Sum 2.2 program was used to calculate group contributions to the molecular orbitals (HOMO and LUMO) and prepare the density of states (DOS) spectrum in Fig. 5. The DOS spectra were created by convoluting the molecular orbital information with GAUSSIAN curves of unit height. The green and red lines in the DOS spectrum indicate the HOMO and LUMO levels.

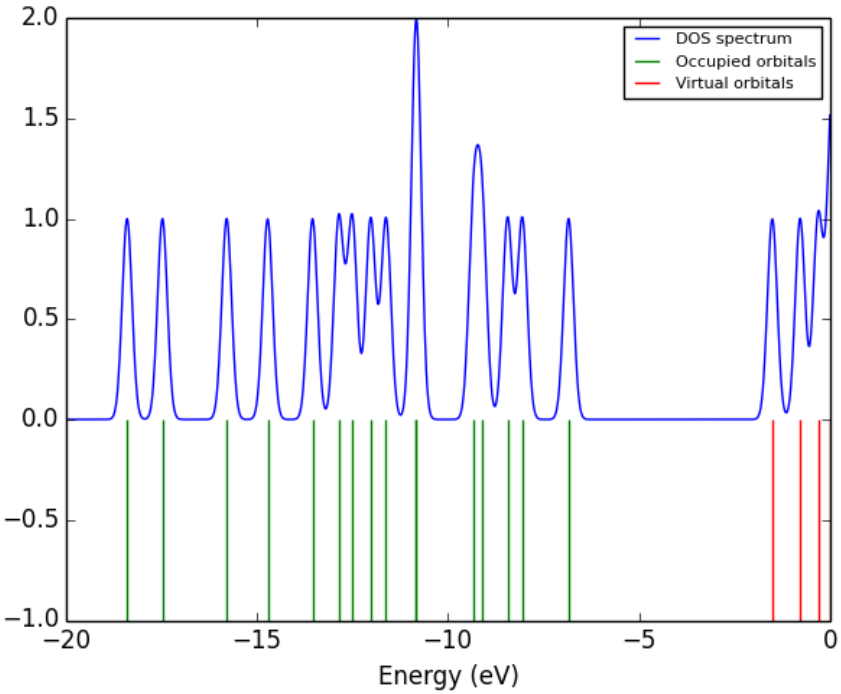

Fig. 5: Density of states (DOS) diagrams for 5-chloro-2-pyridinol

September/October 2020
ISSN: 0193-4120 Page No. 337-357

6. NBO ANALYSIS

The natural bond orbital (NBO) calculation was performed using NBO 3.3 program implemented in the GAUSSIAN 09W package at the B3LYP/6-311++G(d,p) level, in order to understand various second-order interactions between the filled orbitals of one subsystem and vacant orbitals of another subsystem, which is a measure of the delocalization or hyper conjugation. A useful aspect of the NBO method is that it gives information about interactions in both filled and virtual orbital spaces that could enhance the analysis of intra and intermolecular interactions. The second order Fock matrix was carried out to evaluate the donor-acceptor interactions in the NBO analysis [36]. The interactions result in the loss of occupancy from the localized NBO of the idealized Lewis structure into an empty non-Lewis orbital. For each donor (i) and acceptor (j), the stabilization energy $E^{(2)}$ associated with the delocalization (i,j) is estimated as

$$E^{(2)} = \Delta E_{ij} = q_i \frac{F(i,j)^2}{\varepsilon_j - \varepsilon_i} \quad \text{... (2)}$$

where q_i is the donor orbital occupancy and ε_i and ε_j are diagonal elements and F(i,j) is the off diagonal NBO Fock matrix element. Natural bond orbital analysis provides an efficient method for studying intra and intermolecular bonding and interaction among bonds, and also provides a convenient basis for investigating charge transfer or conjugative interaction in molecular systems. Some electron donor orbital, acceptor orbital and the interacting stabilization energy resulted from the second order micro-disturbance theory are reported. The larger the $E^{(2)}$ value is the more intensive will be the interaction between electron donors and electron acceptors, i.e. the more donating tendency from electron donors to electron acceptors, the greater the extent of conjugation of the whole system. Delocalization of electron density between occupied Lewis-type (bond or lone pair) NBO orbitals and formally unoccupied (antibond or Rydgberg) non-Lewis NBO orbitals correspond to a stabilizing donor-acceptor interaction. The intramolecular interactions are formed by the orbital overlap between bonding C–C, C–N, and antibonding C–N orbital, which results in intramolecular charge transfer (ICT) causing stabilization of the system for CP as shown in Table 4. The strong intramolecular hyperconjugative interaction of σ(C–C) to the anti σ*(C–C) bond of the ring leads to stabilization of some part of the ring as obvious from Table 4. For example, the intramolecular hyper conjugative interaction of σ(C3–C4), distribute to σ*(N1–C2) and σ*(C5–C6) leading to stabilization of 27.77 and 15.94 kJ/mol, respectively. This enhanced further to conjugate with antibonding.

This strong stabilization denotes the larger delocalization. The interesting interactions in CP compound is σ(N1–C2) with that of anti-bonding C5–C6. This interaction results in the stabilization energy of 27.87 KJ/mol. This highest interaction around the ring can induce the large bioactivity in the compound.

The angular properties of the natural hybrid orbital (NHO) are also analyzed by NBO analysis which is shown in Table 5. The direction of a hybrid is represented in terms of the polar and azimuthal angles of the vector describing its p-component. The hybrid direction is compared with the direction of the line of centers between the two nuclei to determine the

September/October 2020
ISSN: 0193-4120 Page No. 337-357

bending of the bond. In the CP compound, the chlorine NHO of the πCCl bond is bent away from the line of C–Cl centers by 2.3, whereas the carbon NHO is approximately aligned with C–Cl axis.

7. PREDICTION OF FIRST HYPERPOLARIZABILITY – A NLO PROPERTY

There is an intense current research activity in the area of molecular linear and non-linear optics, devoted to the search for efficient, stable, simple organic compounds exhibiting large hyper polarizabilities. Aromatic backbone compounds are still common and show large non-linear optical properties. Organic non-linear materials have allured a keen interest in recent years, owing to their potential applications in various photonic technologies. Significant effects have focused on studying the electronic and structural properties of donor–acceptor substituted π-conjugated organic compounds with large molecular non-linear optical (NLO) response (β-first-order hyperpolarizability) [37]. Two factors are attributed to NLO properties of such compounds in an electric field: the altered ground state charge distribution by the donor and acceptor moieties and the enhanced-π-electronic charge redistribution through the π-conjugation. The first hyperpolarizability β is associated with the intramolecular charge transfer (ICT), resulting from the electron cloud movement through the π-conjugated framework from electron donor to acceptor groups. The electron cloud is capable of interacting with an external electric field and thereby altering the dipole moment and the first hyperpolarizability.

A reliable prediction of molecular hyperpolarizability requires adequate basis sets and therefore must involve both the diffuse on and polarization functions. As the basis becomes larger, one expects a better description of the compound and accordingly, more accurate results. In the view of these points, B3LYP/6-311++G(d,p) and B3LYP/3-21G method is used for the present study in order to see the effect of the level of theory and basis set. The title compound was fully optimized at B3LYP/ 6-311++G(d,p) method in the GAUSSIAN 09W program. The tensor component of the static first hyperpolarizabilities, β, was analytically calculated by using the same method as mentioned above. From the computed tensorial component β, β_{vec} is calculated for the title compound by taking into account the Kleinman symmetry relations and the squared norm of the Cartesian expression for the β tensor [38].

The components of β are defined as the coefficients in the Taylor series expansion of the energy in the external electric field. When the electric field is weak and homogeneous, this expansion becomes

$$E= E^0 - \mu_\alpha F_\alpha - 1/2\alpha_{\alpha\beta}F_\alpha F_\beta - 1/6\beta_\alpha\beta_\gamma F_\alpha F_\beta F_\gamma + \ldots\ldots$$

where E^0 is the energy of the unperturbed molecules, F_α is the field at the origin and μ_α, $\alpha_{\alpha\beta}$ and $\beta_\alpha\beta_\gamma$ are the components of dipole moment, polarizability and the first hyperpolarizabilities, respectively. The total static dipole moment μ, the mean polarizability α_0 and the mean first hyperpolarizability β, using the x, y, z components are defined as follows,

$$\mu = (\mu_x^2 + \mu_y^2 + \mu_z^2)^{1/2}$$

$$\alpha = \frac{\alpha_{xx} + \alpha_{yy} + \alpha_{zz}}{3}$$

September/October 2020
ISSN: 0193-4120 Page No. 337-357

$$\alpha = 2^{-1/2}[(\alpha_{xx}- \alpha_{yy})^2 + (\alpha_{yy} - \alpha_{zz})^2 + (\alpha_{zz} - \alpha_{xx})^2 + 6\alpha_{xx}^2]^{1/2}$$

$$\alpha = (\alpha_{xx} + \alpha_{yy} + \alpha_{zz}) / 3$$

$$\Delta\alpha = 1/2[(\alpha_{xx} - \alpha_{yy})^2 + (\alpha_{yy} - \alpha_{zz})^2 + (\alpha_{zz} - \alpha_{xx})^2 + 6\alpha_{xx}^2]$$

$$\beta = (\beta_x^2 + \beta_y^2 + \beta_z^2)^{1/2}$$

and

$$\beta_x = \beta_{xxx} + \beta_{xyy} + \beta_{xzz}$$

$$\beta_y = \beta_{yyy} + \beta_{xxy} + \beta_{yzz}$$

$$\beta_z = \beta_{zzz} + \beta_{xxz} + \beta_{yyz}$$

The calculated first hyperpolarizability(β) for CP is 1.9850×10^{-30} esu, and 3.2070×10^{-30} esu by B3LYP/HF with 6-311++G(d,p) methods, respectively and also Dipole moment (μ), Mean polarizability (α), Anisotropy of the polarizability (Δα), Energy values .The large value of hyperpolarizibility, β which is a measure of the non-linear optical activity of the molecular system, associated with the intramolecular charge transfer, resulting from the electron cloud movement through π conjugated frame work from electron donor to electron acceptor groups. So, the title compound is an attractive object for future studies of nonlinear optical properties.

8. THERMODYNAMIC PROPERTIES

The thermodynamic parameters namely heat capacity, entropy, rotational constants, zero point vibrational energies (ZPVE) of the compound CP is also computed at B3LYP/HF levels using 6-311+G(d,p) basis set . The variation in the ZPVE seems to be insignificant. Standard heat capacities ($C_{p,m}^0$), standard entropies (S_m^0) and standard enthalpy changes (ΔH_T^0) from (100 → 1000K) were obtained and are listed in Table 6. The correlation graphs are shown in Fig. 9 and the corresponding fitting equations are as follows:

$S_m^0 = -2.71724 + 0.105192767T + 51.95421118 \times 10^{-5} T^2$ ($R^2 = 0.999973$)

$C_{p,m}^0 = -0.00017 + 0.392671454T + 9.248527249 \times 10^{-5} T^2$ ($R^2 = 0.999503$)

$\Delta H_m^0 = -4.28353 + 0.093850737T - 2.210447686 \times 10^{-5} T^2$ ($R^2 = 0.999503$)

September/October 2020
ISSN: 0193-4120 Page No. 337-357

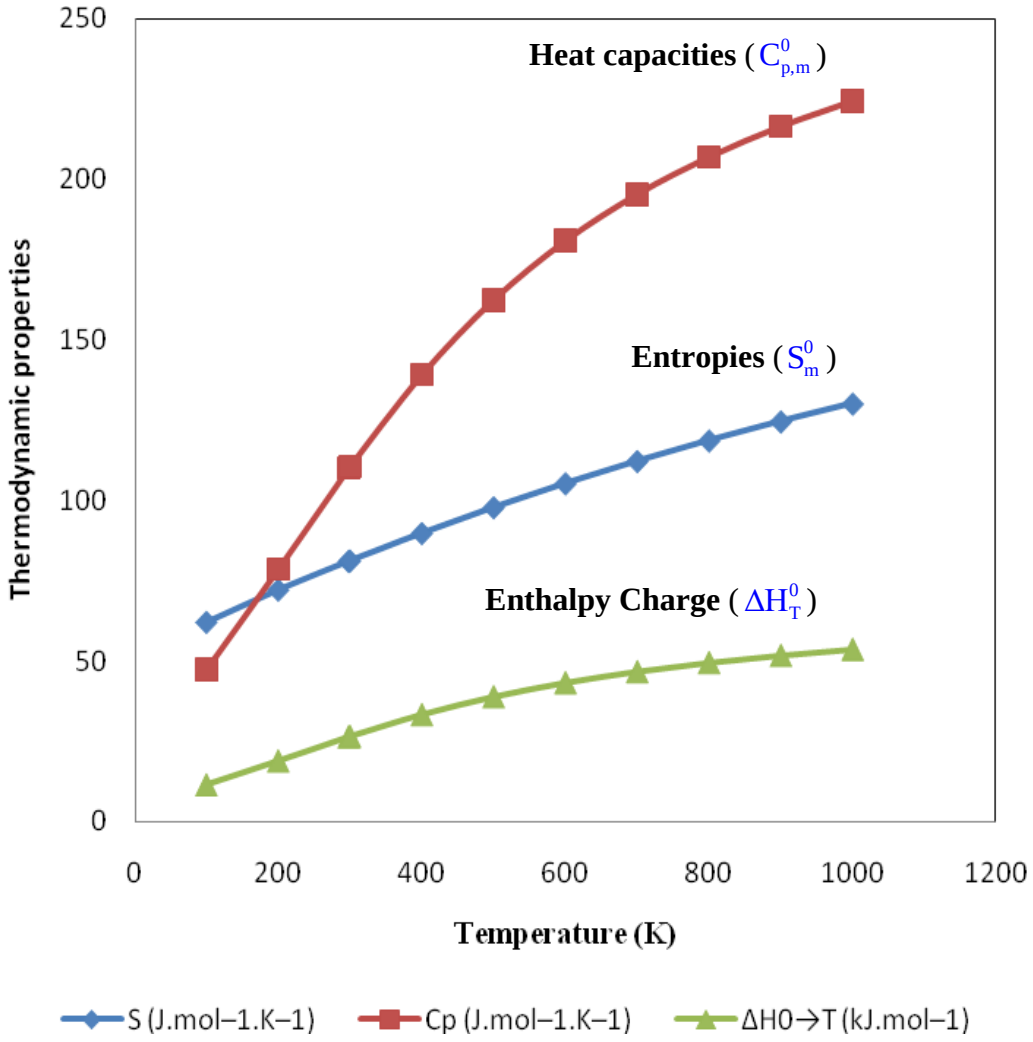

Fig. 9: Temperature dependence of entropy, heat capacity, enthalpy of 5-Chloro-2-Pyridinol

9. CONCLUSION

Attempts are made in the present investigation for the molecular parameters and frequency assignments for CP from the FT-IR and FT Raman spectra. Vibrational frequencies, infrared intensities and Raman activities are calculated and analyzed by *ab initio* HF and DFT (B3LYP) levels of theory utilizing 6-311++G(d,p) higher basis set. The difference between the observed and scaled wavenumber values of most of the fundamentals are very small. Comparison between the calculated and experimental structural parameters indicates that B3LYP results are in good agreement with experimented values. The assignments made at a higher level of theory with higher basis set, with only reasonable deviations from the experimental values seem to be correct. HOMO and LUMO energy gap explains the eventual charge transfer interaction taking place within the molecule. Also the molecular electrostatic potential map shows that the negative potential sites are on the electronegative atoms and the positive potential sites are around the hydrogen atoms. These sites give relevant information

September/October 2020
ISSN: 0193-4120 Page No. 337-357

about the possible areas for inter- and intramolecular hydrogen bonding. Natural bond orbital analysis indicates the strong intramolecular interactions. Natural bond orbital analysis of CP confirms that the intramolecular charge transfer caused by p-electron cloud movement from donor to acceptor must be responsible for the non-linear optical properties of the title compound. The correlations between the thermodynamic properties $C^0_{p,m}$, S^0_m and ΔH^0_m vs temperature T are also obtained.

Table 1: Optimized geometrical parameters of 5-chloro-2-pyridinol obtained by B3LYP/6-311++G(d,p) and HF/6-311++(d,p) level calculations

Bond Length	Value (Å)		Bond angle	Value (◦)		Dihedral Angle	Value (◦)	
	B3LYP/ 6-311++G(d,p)	HF/ 6-311++G(d,p)		B3LYP/ 6-311++G(d,p)	HF/ 6-311++G(d,p)		B3LYP/ 6-311++G(d,p)	HF/ 6-311++G(d,p)
N1-C2	1.3255	1.3044	C2-N1-C6	118.3916	118.5596	C6-N1-C2-C3	-0.0026	0.0068
N1-C6	1.3383	1.3277	N1-C2-C3	123.6871	123.6858	C6-N1-C2-O7	180.0069	180.0081
C2-C3	1.4008	1.3965	N1-C2-O7	117.6986	118.0912	C2-N1-C6-C5	0.0045	0.0034
C2-O7	1.3523	1.3316	C3-C2-O7	118.6143	118.223	C2-N1-C6-H12	-179.997	-179.999
C3-C4	1.3841	1.3704	C2-C3-C4	117.7671	117.5571	N1-C2-C3-C4	-0.0007	-0.0119
C3-H9	1.0819	1.0725	C2-C3-H9	120.2742	120.1547	N1-C2-C3-H9	179.9957	179.9871
C4-C5	1.3961	1.3917	C4-C3-H9	121.9588	122.2881	O7-C2-C3-C4	-180.01	179.9868
C4-H10	1.0828	1.0742	C3-C4-C5	118.7254	118.8725	O7-C2-C3-H9	-0.0138	-0.0142
C5-	1.3873	1.3708	C3-	120.8906	120.8375	N1-	0.04	-0.0116

Published by: The Mattingley Publishing Co., Inc.

September/October 2020
ISSN: 0193-4120 Page No. 337-357

C6			C4-H10			C2-O7-H8		
C5-Cl11	1.7541	1.7409	C5-C4-H10	120.384	120.29	C3-C2-O7-H8	180.0489	-180.01
C6-H12	1.0844	1.0745	C4-C5-C6	119.2361	118.7925	C2-C3-C4-C5	0.002	0.0069
O7-H8	0.9674	0.9443	C4-C5-Cl11	120.6013	120.6807	C2-C3-C4-H10	179.9981	180.0013
			C6-C5-Cl11	120.1626	120.5267	H9-C3-C4-C5	-179.994	-179.992
			N1-C6-C5	122.1928	122.5324	H9-C3-C4-H10	0.0018	0.0022
			N1-C6-H12	116.9661	116.7068	C3-C4-C5-C6	-0.0002	0.0022
			C5-C6-H12	120.8412	120.7608	C3-C4-C5-Cl11	-179.999	179.9959
			C2-O7-H8	107.0274	108.74	H10-C4-C5-C6	-179.996	-179.992
						H10-C4-C5-Cl11	0.0045	0.0015
						C4-C5-C6-N1	-0.0032	-0.0078
						C4-	179.9986	179.9941

TEST Engineering & Management

September/October 2020
ISSN: 0193-4120 Page No. 337-357

						C5-C6-H12		
						Cl11-C5-C6-N1	179.996	179.9985
						Cl11-C5-C6-H12	-0.0022	0.0005

Table 2: The observed FT-IR, FT-Raman and calculated (Unscaled and Scaled) frequencies (cm^{-1}) and probable assignments (Characterized by TED) of 5-chloro-2-pyridinol using HF/6-311++G(d,p) and B3LYP/6-311++G(d,p) methods and basis set

No.	Symmetry Species	Observed frequency (cm^{-1})		Calculated frequency (cm^{-1})				TED (%)
		FT-IR	FT-Raman	B3LYP/6-311++G(d,p)		HF/6-311++G(d,p)		
				Unscaled	Scaled	Unscaled	Scaled	
1	A_I	3700 vw	-	3780	3707	4141	3692	OH(100)
2	A_I	3133 m	3130 m	3211	3105	3377	3113	CH(99)
3	A_I	3084 ms	3084 w	3196	3090	3355	3090	CH(99)
4	A_I	3057 s	3035 w	3179	3074	3355	3090	CH(99)
5	A_I	1614 vs	1621 vw	1636	1618	1796	1626	CC(56), bCH(14), CN(11), Rsymd(8)
6	A_I	1554 vs	1548 m	1617	1552	1779	1562	CC(43), CN(27), bCH(11), Rasymd(10)
7	A_I	1470 s	1472 ms	1500	1467	1642	1470	bCH(48), CC(20), CN(16), CO(12)
8	A_I	1426 s	1426 s	1434	1401	1546	1422	CN(37), CC(20), bCOH(14), bCH(11), bCCl(5), bCO(5)

September/October 2020
ISSN: 0193-4120 Page No. 337-357

9	A_I	1332 ms	1340 vw	1352	1332	1460	1335	bCH(55), bCOH(16), CC(14), CN(10)
10	A_I	-	1267 m	1318	1286	1433	1267	CO(45), CN(19), bCH(18), Rtrigd(12)
11	A_I	1235 m	-	1296	1240	1328	1231	CN(50), CC(32), bCH(14)
12	A_I	1153 m	1158 s	1186	1160	1240	1156	bCOH(39), CC(25), bCH(14), CN(14)
13	A_I	1118 m	1119 vw	1141	1115	1219	1117	bCH(59), CC(20), CN(8), bCOH(7)
14	A_I	992 ms	1040 vs	1118	1095	1180	1070	CC(46), CCl(24), bCH(18), Rtrigd(5)
15	A_I	973 w	990 w	1025	995	1105	997	Rtrigd(56), CN(17), CC(14), bCH(7), CCl(5)
16	A_{II}	920 m	930 w	973	946	1101	978	gCH(90)
17	A_{II}	850 m	842 w	932	906	1061	943	gCH(86), tring(7)
18	A_I	-	826 w	865	843	933	834	CC(28), CO(21), Rasymd(20), Rtrigd(12), CN(11)
19	A_{II}	-	813 s	839	817	926	829	gCH(72), gCO(14), tRsymd(7)
20	A_{II}	668 s	670 w	749	729	833	740	tring(61), gCO(24), gCH(8), gCCl(6)
21	A_I	638 w	643 w	665	646	720	646	CCl(34), Rsymd(22), Rasymd (14), CO(11), Rtrigd(9), CC(6)
22	A_I	616 s	620 s	651	629	700	629	Rsymd(45), Rasymd(31), CC(9), bCO(7)
23	A_{II}	503 w	508 w	542	526	587	522	gCO(25), tRsymd(23), gCCl(21), tring(14), tOH(12)
24	A_{II}	415s	-	479	463	494	439	tOH(57), tRsymd(15), gCCl(11), gCO(11)
25	A_I	-	416 s	441	427	480	434	bCO(60), Rsymd(13), bCCl(9), bCOH(5)
26	A_I	-	-	431	418	472	419	tRasym(83), gCH(12)
27	A_{II}	-	315 ms	387	376	418	376	Rasymd (39), CCl(27), Rsymd(18), CC(7)
28	A_{II}	-	281 vw	320	308	353	314	gCCl(49), tRsymd(14), tring(13), tRasym(9), gCH(9), gCO(6)

Published by: The Mattingley Publishing Co., Inc.

September/October 2020
ISSN: 0193-4120 Page No. 337-357

29	A_I	-	244 vw	260	249	280	252	bCCl(78), bCO(11)
30	A_{II}	-	126 ms	121	117	137	122	tRsymd(74), gCCl(12), gCH(10)

Abbreviations: b-bending; g-out-of-plane bending; t-torsion; R-ring;; asym-assymetic; sym-symmetric; vs-very strong; s-strong; ms-medium strong; m-medium; w-weak; vw-very weak.

Table 3: HOMO-LUMO energy and other related properties of 5-chloro-2-pyridinol in a.u. based on B3LYP/6-311++G(d,p) and HF/6-311++G(d,p) methods

Parameters	B3LYP/6-311++G(d,p)	HF/6-311++G(d,p)
HOMO	-0.28463	-0.35130
LUMO	-0.01811	0.14572
Global Hardness (η)	-0.13326	-0.24851
Electronegativity (χ)	-0.15137	-0.10279
Global softness (s)	-7.50412	-4.02398
Chemical potential (μ)	0.15137	0.10279
Global Electrophilicity (ω)	-0.08597	-0.02125

Table 4: Second order perturbation theory of Fock matrix in NBO basis using B3LYP/6-311++G(d,p) basis set for 5-chloro-2-pyridinol

Donor NBO (i)	Acceptor NBO (j)	Occupancy	E(2) j K/mol	E(j) – E(i) a.u.	F(i, j) a.u.
σ(N1-C2)	σ*(C3-C4)	1.98542	10.48	0.34	0.053
σ(N1-C2)	σ*(C5-C6)	1.72665	27.87	0.32	0.087
σ(C3-C4)	σ*(N1-C2)	1.97008	27.77	0.27	0.079
σ(C3-C4)	σ*(C5-C6)	1.70220	15.94	0.28	0.06
σ(C5-C6)	σ*(N1-C2)	1.98454	12.88	0.28	0.055
σ(C5-C6)	σ*(C3-C4)	1.69021	22.77	0.3	0.074
π(C3-H9)	π*(N1-C2)	1.97815	4.61	1.07	0.063
π(C6-H12)	π*(N1-C2)	1.98147	4.09	1.07	0.059
π(C6-H12)	π*(C4-C5)	1.98144	4.08	1.08	0.059
π(O7-H8)	π*(C2-C3)	1.98587	4.56	1.28	0.068
LP_1N1	σ*(C2-C3)	1.90051	9.75	0.89	0.084
LP_2O7	σ*(N1-C2)	1.85572	35.13	0.32	0.103
LP_3Cl11	σ*(C5-C6)	1.93529	12.16	0.32	0.060
σ*(N1 - C2)	σ*(C3-C4)	1.96844	152.95	0.02	0.085

November/December 2020
ISSN: 0193-4120 Page No. 337-357

σ*(N1 - C2)	σ*(C5-C6)	1.66537	296.06	0.01	0.079
σ*(C5 - C6)	σ*(C3-C4)	1.67732	224.42	0.01	0.078

Table 5: The angular properties of natural hybrid orbitals (NHO) of 5-chloro-2-pyridinol using B3LYP at 6-311++G(d,p) basis set

NBO	Line of Centers		Hybrid 1			Hybrid 2		
	Theta	Phi	Theta	Phi	Dev	Theta	Phi	Dev
π(N1-C2)	90	118.5	--	--	--	90	295	3.6
σ(N1-C2)	90	118.5	0	0	90	0	0	90
π(N1-C6)	90	0.1	90	358.5	1.6	90	176.5	3.7
π(C2-C3)	90	62.2	90	66.1	3.9	--	--	--
π(C2-O7)	90	180.8	90	182.5	1.7	--	--	--
σ(C3-C4)	90	0	0	0	90	0	0	90
π(C4-C5)	90	298.7	--	--	--	90	115.6	3.1
π(C5-C6)	90	237.9	90	240.7	2.7	90	59.8	1.8
σ(C5-C6)	90	237.9	0	0	90	0	0	90
π(O7-H8)	90	253.8	90	250.3	3.5	--	--	--
σ*(N1-C2)	90	118.5	0	0	90	0	0	90
σ*(C3-C4)	90	0	0	0	90	0	0	90
σ*(C5-C6)	90	237.9	0	0	90	0	0	90

Table 6: Temperature dependence of the thermodynamic properties of 5-chloro-2-pyridinol determined by DFT/B3LYP 6-311++G(d,p) method

T(K)	5-chloro-2-hydroxypyridine		
	S ($J.mol^{-1}.K^{-1}$)	Cp ($J.mol–1.K^{-1}$)	$\Delta H_0 \rightarrow T$ ($kJ.mol^{-1}$)
100	61.98136	47.45	11.34082
200	72.06262	78.7	18.80975
298.15	80.98709	110.11	26.31692
300	81.14962	110.68	26.45315
400	89.72036	139.18	33.26482
500	97.7653	162.48	38.83365
600	105.2486	180.86	43.22658
700	112.1821	195.36	46.69216
800	118.6066	206.98	49.46941
900	124.5674	216.48	51.73996
1000	130.1195	224.37	53.62572

References

1. Gilchrist T L, Heterocylic Chemistry, John Wiley & Sons, New York, 1988.

November/December 2020
ISSN: 0193-4120 Page No. 337-357

2. Fallas J A, Gonzalez L, Corral I, Journal of Tetrahedron Letters, 65 (2009) 232.
3. Zucchi F, Trabanelli G, Gonzalez N A, Journal of Archaeological Modern Chemistry, 132 (1995) 4579.
4. Khan B T, Khan S R A, Annapoorna K, Indian Journal of Chemical Society, 34 (1995) 11878.
5. Lizarraga M E, Navarro R, Urriolabeitia E P, Journal of Organo Metallic Chemistry, 542 (1997) 51.
6. Georgopoulou A S, Ulvenlund S, Mingos D M P, Baxter I, Williams D J, Journal of Chemical Society, 4 (1999) 547.
7. Liaw W, Lee N, Chen C, Lee C, Lee G, Peng S, Journal of American Chemical Society, 122 (2000) 488.
8. Trotter P J, White P A, Journal of Applied Spectroscopy, 32 (1978) 323.
9. Rajpure K Y, Bhosale C H, Journal of Materials Chemistry and Physics, 64 (2000) 70.
10. Licht S, Journal of Solar Energy Materials and Solar Cells, 38 (1995) 305.
11. Altenburger J M, Lassalle G Y, Matrougui M, Galtier D, Jetha J C, Bocskei Z, Berry C N, Lunven C, Lorrain J, Herault J P, Schaeffer P, O'Connor S E, Herbert J M, Bioorganic and Medicinal Chemistry Letters, 12 (2004) 1713.
12. Camp H, Perk J, Hand Book of American Chemical Society (2000) 31.
13. Murugan R, Scrivan E F V, Aldrichim Acta 36 (2003) 21.

A. Topacli, S. Bayari, Spectrochim. Acta Part A 57 (2001) 1385.

14. R.N. Medhi, R. Barman, K.C. Medhi, S.S. Jois, Spectrochim. Acta Part A 56 (2000) 1523.
15. Sujin P Jose, Mohan S, Spectrochimica Acta Part A 64 (2006) 240.
16. Becke A D, Physics Review A 38 (1988) 3098.
17. A.D. Becke, J. Chem. Phys., 98 (1993) 5648.
18. C. Lee, W. Yang, R.G. Parr, Phys. Rev., B37 (1988) 785.
19. M.J. Frisch, G.W. Trucks, H.B. Schlegal, G.E. Scuseria, M.A. Robb, J.R. Cheesman, V.G. Zakrzewski, J.A. Montgomerg, Jr., R.E. Stratmann, J.C. Burant, S. Dapprich, J.M. Millam, A.D. Daniels, K.N. Kudin, M.C. Strain, O. Farkas, J. Tomasi, V. Barone, M. Cossi, R. Cammi,B. Mennucci, C. Pomelli, C. Adamo, S. Clifford, J. Ochterski, G.A. Petersson, P.Y. Ayala, Q. Cui, K. Morokuma, N. Rega, P. Salvador, J.J. Dannenberg,D.K. Malich, A.D. Rabuck, K. Raghavachari, J.B. Foresman, J. Cioslowski,J.V. Ortiz, A.G. Baboul, B.B. Stetanov, G. Liu, A. Liashenko, P. Piskorz,I. Komaromi, R. Gomperts, R.L. Martin, D.J. Fox, T. Keith, M.A. Al-Laham,C.Y. Peng, A. Nanayakkara, M. Challacombe, P.M.W. Gill, B. Johnson,W. Chen, M.W. Wong, J.L. Andres, C. Gonzalez, M. Head-Gordon,E.S. Replogle, J.A. Pople, GAUSSIAN 09, Revision A 11.4, Gaussian, Inc,Pittsburgh PA, 2009

(a) T. Sundius, J. Mol. Struct., 218 (1990) 321.
(b) MOLVIB (V.7.0): Calculation of Hormonic Force Fields and Vibrational Modes of Molecules, QCPE program No.807 (2002).

20. P.L. Polavarapu, J. Phys. Chem. **94** (1990) 8106.

21. Sundius T, Vibr. Spectrosc., 29 (2002) 89
22. G. Fogarasi, P. Pulay, in: J.R. During (Ed.), Vibrational Spectra and Structure, Vol.14, lsevier, Amsterdam, Chapter 3, (1985) PP. 125-219
23. G. Keresztury, S. Holly, J. Varga, G. Besenyei, A.Y. Wang, J.R. Durig, Spectrochim. Acta Part A **49** (1993) 2007.
24. Keresztury G, Raman Spectroscopy: Theory in: J.M. Chalmers, P.R. Griffiths (Ed.), Handbook of Vibrational Spectroscopy, Vol. 1, Wiley, 2002.
25. G. Socrates, Infrared and Raman Characteristic Group Frequencies – Tables and Charts, Third ed, Wiley, New York, 2001.
26. Silverstein R M, Clayton Basseler G, Morrill, Spectrometric identification of Organic Compounds, John Wiley and Sons, New York, 1991.
27. Varsanyi, Assignment for vibrational Spectra of seven Hundred Benzene Derivatives, Vol. 1-2, Academic Kiaclo, Budapest, 1973.
28. Dwivedi C P D, Sharma S N, Indian J. Pure Appl. Phys. 11 (1973) 447.
29. Gunasekaran S, Seshadri S, Muthu S, Indian J. Pure Appl. Phys., 44 (2006) 581.
30. Jag Mohan, Organic Spectroscopy - Principles and Applications, second ed., Narosa, Publishing House, New Delhi, 2001.
31. Balamurugan N, Charanya C, Sampath Krishnan S, Muthu S, Spectrochim. Acta A 137 (2015) 1374.
32. T. Vijayakumar, I. Hubert Joe, C.P.R. Nair, V.S. Jayakumar, Chem. Phys. **343** (2008) 83.
33. Kandasamy M, Velraj G, Kalaichelvan S, Mariappan G, Spectrochim. Acta Part A, 134 (2015) 191.
34. Arivazhagan M et al., Spectrochimica Acta, Part A: Molecular and Biomolecular Spectroscopy, 104 (2013) 14.
35. V. Krishnakumar, N. Prabavathi, Spectrochimica Acta 72A (2009) 738.
36. D.A. Kleinman, Phys. Rev. **126** (1962) 1977.